Neoplasma 2022; 69(6): 1303–1313

doi:10.4149/neo_2022_220609N615

HOXC10 indicates poor survival outcome in gastric cancer and promotes G1/S cell cycle transition through transcriptional repression of p21

Zheng-Hua LIN[1,2,3], Jia-Min HE[2,4], San-Chuan LAI[1,2,3], Ning DING[1,2,3], Ying JIANG[1], Xing-Kang HE[2,4], Xiao-Sun LIU[5], Zhi-Hui HUANG[4,*]

[1]Department of Gastroenterology, The Second Affiliated Hospital, School of Medicine, Zhejiang University, Hangzhou, Zhejiang, China; [2]Institute of Gastroenterology, Zhejiang University, Hangzhou, Zhejiang, China; [3]Zhejiang University Cancer Center, Hangzhou, Zhejiang, China; [4]Department of Gastroenterology, Sir Run Run Shaw Hospital, School of Medicine, Zhejiang University, Hangzhou, Zhejiang, China; [5]Department of Gastroenterology, The First Affiliated Hospital, School of Medicine, Zhejiang University, Hangzhou, Zhejiang, China

**Correspondence: zhihui808@zju.edu.cn*

Received June 9, 2022 / Accepted October 8, 2022

Homeobox (HOX) genes encode proteins that function as transcription factors during embryogenesis and tumorigenesis. We have previously reported upregulation of HOXC10 in gastric cancer (GC) tissues using cDNA microarray analysis. Though the functional role of HOXC10 in GC has been briefly reported, its specific mechanism is not fully understood. We analyzed the expression of HOXC10 in GC tissues, as well as its correlation with the survival outcome. By in vitro and in vivo assays, we further investigated the role of HOXC10 on cell cycle control and proliferation. Finally, we screened potential downstream targets of HOXC10 by cDNA microarray and explored the role of HOXC10 in p21 transcriptional repression through a dual luciferase reporter and chromatin immunoprecipitation. We illustrated the upregulation of HOXC10 in GC tissues and high HOXC10 expression related to poor survival outcome. Multivariable COX regression analysis showed that HOXC10 was an independent predictor of survival (HR=1.863; 95% CI: 1.076–3.225). Functionally, HOXC10 could promote GC cell proliferation and tumor growth in nude mice. Overexpression of HOXC10 accelerated G1/S cell cycle transition, whereas knocking down HOXC10 induced cell cycle arrest at the G1 phase. Critical factors of G1/S cell cycle transition including p21, CDK2, and c-Myc, were regulated by HOXC10. Importantly, an inverse correlation between p21 and HOXC10 expression in GC cell lines and tissues was observed. HOXC10 could directly bind to the promoter region of p21 and repress its transcriptional activity. Collectively, we identified HOXC10 as a predictor of poor prognosis in GC patients, and a novel transcriptional regulator of p21 in the G1/S cell cycle transition.

Key words: HOXC10; gastric cancer; cell cycle; p21; transcriptional regulation

Gastric cancer (GC) is one of the most commonly diagnosed malignancies and the fourth leading cause of cancer-related mortality worldwide [1]. Despite extensive efforts in improving outcomes, the five-year survival of GC remains very low at approximately 20% [2]. Multiple factors contribute to the tumorigenesis and progression of GC, which is characterized as a highly heterogeneous tumor. Although several driver genes, including HER-2 and TP53, have been identified [3], effective prognostic indicators and therapeutic targets in GC have not been established to date. Thus, understanding the molecular mechanisms of genetic aberrations in GC is critical for predicting survival outcomes and developing therapeutic strategies.

The homeobox (HOX) gene was first identified to be associated with segmental development of the *Drosophila* in 1984 [4], and the counterparts in humans, including A, B, C, and D clusters, are widely accepted to be vital regulators from embryogenesis to carcinogenesis [5]. Studies have identified the involvement of HOX genes in the progression of various solid tumors, including breast cancer [6], colorectal cancer [7], liver cancer [8], prostate cancer [9], and lung cancer [10]. The aberrant expression of HOX genes in GC tissues have been correlated to patient survival [11, 12]. Recent studies have reported that overexpression of HOXC10 in GC contributes to cell proliferation and migration, suggesting a strong biological involvement of HOXC10 in GC progression [13–15]. However, the functional roles and underlying molecular mechanisms of HOXC10 in GC has not been fully elucidated.

We have previously screened the differential expression of genes in GC and matched non-malignant tissues by cDNA microarray and found that HOXC10 is upregulated in GC tissues [16]. HOXs encode transcription factors that regulate the expression of target genes at the transcriptional level and play critical roles in tumorigenesis and cancer progression [17]. HOXC10 has been demonstrated to enhance DNA

damage repair and facilitate the G1 to S phase cell cycle transition by binding to and activating cyclin-dependent kinase (CDK) 7 in breast cancer cells [18]. In this study, we identified HOXC10 as an independent prognostic factor for GC patient survival and a regulator of p21 expression. p21 is encoded by the CDKN1A gene, and earlier studies have shown that its transcription is controlled by p53 and p53-independent modes [19]. As a member of cyclin-dependent kinase inhibitors, p21 plays an important role in cell cycle regulation and carcinogenesis [20, 21]. Interestingly, our results revealed that HOXC10 was physically bound to the p21 promoter and inhibited the transcriptional activity of p21. Upregulation of HOXC10 in GC promoted cell proliferation and G1/S cell cycle transition by transcriptionally repressing the expression of p21.

Patients and methods

Patients. Primary GC and matched adjacent non-tumor tissues were obtained from patients at Sir Run Run Shaw Hospital (clinical cohort 1) and the First Affiliated Hospital (clinical cohort 2) of Zhejiang University. None of the patients had received preoperative treatments such as radiotherapy or chemotherapy. The median follow-up of patients in clinical cohort 2 was 44.3 months. The study protocol was approved by the Clinical Research Ethics Committee of the Second Affiliated Hospital of Zhejiang University and informed consent was obtained from all individual participants included in the study.

Tissue microarray and immunohistochemical staining. Tumor samples were obtained from 195 patients with primary GC who underwent surgery at the First Affiliated Hospital of Zhejiang University (clinical cohort 2) from March 2010 to May 2013. The human GC immunohistochemistry tissue microarray was performed according to standard technologies as described previously (in collaboration with Superchip Company, Shanghai, China) [39]. Immunohistochemistry was performed with an anti-HOXC10 antibody (ab153904, Abcam, UK). Protein expression was quantified by two experienced pathologists blinded to the clinical data and based on the extent of staining (the proportion of positive cells, 0: 0–5%; 1: 6–50%; 2: 51–75%; 3: 76–100%) and the intensity of staining (0: no staining; 1: weak staining; 2: moderate staining; 3: strong staining) [39]. Then, the extent of staining multiplied by the intensity grades was used to define HOXC10 protein expression which was classified into two categories: high level (grades 3–9) and low level (grades 0–2).

Cell culture. The human GC cell lines (BGC823, HGC27, MGC803, SGC7901, AGS, MKN28, and MKN45) and normal gastric epithelial cell line (GES-1) were obtained from Riken Gene Bank (Tsukuba, Japan), China Infrastructure of Cell Line Resource (Beijing, China), and American Type Culture Collection (ATCC, Manassas, VA, USA). All of the cell lines were routinely cultured in the recommended culture conditions and incubated at 37 °C in a humidified environment containing 5% CO_2.

Cell transfection. AGS, MKN28, and HEK-293T cell lines were transfected with pcDNA3.1-HOXC10 or pcDNA3.1 empty vector using Lipofectamine 3000 Reagent (Invitrogen, Shanghai, China). For HOXC10 knockdown, shRNAs (pGPU6/GFP/Neo) or siRNAs for HOXC10 and the corresponding control oligonucleotides (scramble shRNA or siRNA) were purchased from GenePharma (GenePharma, Shanghai, China). To generate GC cells with stable HOXC10 overexpression or knockdown, transfected cells were selected by 400 μg/ml G418 (Sigma, MO, USA) for another 14 days. The transfection of BGC823 and SGC7901 cells were performed with Lipofectamine RNAiMAX Reagent (Invitrogen, Shanghai, China) following the manufacturer's instruction. The sense sequences of HOXC10 shRNA were as follows: SH-1(SH) 5'-GATCCCGGAGATTAGCAAGATCATTAATGTGCTGTCTTAATGGTCTTGCTAATCTCCTTTTTA-3', SH-2 5'-GATCCCCGAAGCGAAAGAGGAGATAAATGTGCTGTCTTTATCTCCTCTTTCGCTTCGTTTTTA-3'. The sense sequences of HOXC10 siRNA were as follows: Si-1 5'-GCAGGCAUGUAUAUGCAGUTT-3', Si-2 5'-CGGAUAACGAAGCGAAAGATT-3', Si-3 5'-CGCAGAAUGAAACUCAAGATT-3'.

Quantitative real-time PCR (qRT-PCR). Total RNAs from tissues and cultured cells were extracted with TRIzol reagent (Invitrogen, Shanghai, China) following the manufacturer's protocols. Total RNA was reversely transcribed to cDNA using a Reverse Transcription Kit with gDNA Eraser (RR047A, Takara). qRT-PCR was performed with SYBR Premix Ex Taq II Kit (RR820A, TaKaRa) in a LightCycler480 System. PCRs were repeated in triplicate. GAPDH was used as an endogenous control in cells and snRNA U6 in tissues. The primers used are shown in Supplementary Table S5.

Western blotting. Proteins were extracted with RIPA reagent (Beyotime, Beijing, China) supplemented with a protease inhibitor cocktail (Roche, CA, USA). Total proteins were loaded on 10% SDS-PAGE gel and electrophoretically transferred to PVDF membranes. Membranes were blocked with 5% skimmed milk and incubated overnight at 4 °C with primary antibodies. We used 1:1000 anti-HOXC10 polyclonal antibody (ab153904; Abcam, UK), 1:1000 anti-p21 antibody (ab109520; Abcam, UK), 1:1000 anti-Cdk2 antibody (ab32147; Abcam, UK), 1:1000 c-Myc antibody (#9402; Cell Signaling Technology, USA), 1:500 anti-β tubulin antibody (ab134175; Abcam, UK), and 1:10000 anti-human GAPDH antibody (ab181602; Abcam, UK). GAPDH or β-tubulin was used as an endogenous control.

Colony formation and cell growth assays. Cells with stable overexpression or knockdown of HOXC10 were trypsinized into single-cell suspension and plated in 6-well plates. At the endpoint, colonies were fixed with methanol and stained with 0.1% crystal violet (Sigma, MO, USA) for 30 min. The colony formation was determined by counting the number of stained colonies. For cell growth curve assays;

3,000 transfected cells/well were seeded onto the 96-well plates. After 6 h of culture, as well as at 24 h, 48 h, 72 h, and 96 h, cells were measured using Cell Counting Kit-8 (CCK-8, Dojindo, Japan) and the cell growth curves were then obtained. For the EdU incorporation assays, the EdU kit (RiboBio, Guangzhou, China) was used according to the manufacturer's instructions.

Cell cycle analysis. Cells were serum-starved overnight and stimulated with a complete medium for 4 h. Cell cycle was detected by the Cell Cycle Staining Solution Kit (Multi-Sciences, China) and analyzed by flow cytometry. For the cell cycle synchronization, the synchronization drug nocodazole (40 ng/ml) (Beyotime, Beijing, China) was imposed on HOXC10-depleted BGC823 cells for 12 h to block the majority of cells in the G2/M phase. DMSO treatment was used as an unsynchronized control. 0 h, 4 h, and 8 h after release from the nocodazole block, cell cycle distribution was detected.

Cell migration and invasion assay. Cell migration was assessed by Transwell chambers assay (Corning, NY, USA). Briefly, 5×10^4 cells were plated into 200 μl of 1% FBS medium in the upper chamber with 600 μl of 10% FBS medium added to the lower chamber. Cells were incubated for 18–24 h. Then, cells on the bottom of the membrane were fixed and stained with DAPI. For cell invasion assay, Matrigel-coated Transwell chambers were prepared 6 hours before the seeding of cells. $1.5–3\times10^5$ cells were plated into 200 μl of 1% FBS medium in the upper chamber with 600 μl of a medium containing 10% FBS in the lower chamber. After 24 h, cells and Matrigel in the upper inserts were discarded and cells on the bottom of the membrane were fixed and stained with 0.1% crystal violet (Sigma, MO, USA).

Subcutaneous xenograft mice models. For subcutaneous xenografts, MKN28 cells with stable overexpression of HOXC10 and BGC823 cells with stable depletion of HOXC10 shRNA were injected subcutaneously into the flanks of athymic nude mice. Six 5-week-old male nude mice were used in each group. 150 μl of cell suspension and matrix gum mixture containing $4–8\times10^6$ cells were injected subcutaneously into nude mice. Tumor size was measured every 3 days using a digital caliper. At the endpoint, tumors were harvested and measured. The nude mice were achieved from the Experimental Animal Center of Zhejiang University and the study protocols were approved by the Animal Ethics Committee of the Second Affiliated Hospital of Zhejiang University, all institutional and national guidelines for the care and use of laboratory animals were followed.

Immunohistochemistry. Tissue samples were fixed in a 4% formaldehyde solution and embedded in paraffin. Antigen retrieval was enforced in citrate buffer (pH 6.5) for 5 min. Tissue slices were incubated overnight at 4 °C with primary antibodies and followed by secondary antibody incubation using Immunohistochemical Secondary Antibody Kit (ZSGB-Bio, Beijing, China). Antigen-antibody complexes were then determined with a DAB kit (ZSGB-Bio, Beijing, China). Slices were lightly counterstained with hematoxylin to visualize nuclei.

Luciferase assay. The DNA fragment containing the promoter region (–2.5 kb~+180 bp) of the p21 gene (CDKN1A, Gene Bank Number NG_009364.1) was synthesized and cloned into pGL3-basic (Promega, Madison, USA) vector between the MluI and XhoI sites to obtain pGL3-p21-promoter. 5×10^4 HEK-293T cells were seeded in 24-well plates for 18 h, then transfected with 0.5 μg pcDNA3.1 empty vector or pcDNA3.1-HOXC10, 0.5 μg pGL3-basic empty vector or pGL3-p21-promoter, and 0.06 μg pRL-TK vector (Promega) using Fugene HD (Promega). Meanwhile, BGC823 cells were transfected with 0.5 μg control shRNA or HOXC10 shRNA, 0.5 μg pGL3-basic empty vector or pGL3-p21-promoter, and 0.06 μg pRL-TK vector. 72 h after transfection, luciferase activity was detected by the dual-luciferase reporter assay system (Promega) following the manufacturer's protocols.

Chromatin immunoprecipitation (ChIP) assay. The ChIP assays were performed using the EZ-Magna ChIP™ A/G kit (Millipore, MA, USA), according to the manufacturer's instructions. Briefly, HEK-293T and BGC823 cells transfected with GV141-HOXC10 plasmid (GenePharma, Shanghai, China) were cross-linked by the addition of formaldehyde, sonicated, and used for immunoprecipitation with an anti-Flag antibody. Normal Mouse IgG was used as a negative control. PCR primers used to amplify 223 bp DNA fragment specific to the p21 promoter were as follows: Forward 5'-TGATGCGCTCTGTTACGT-3', Reverse 5'-CTGGCAATCTACAACCTGTC-3'.

Statistical analysis. Statistical analysis was performed using the GraphPad Prism 6.0 software (GraphPad Software, CA, USA) and the SPSS 22.0 software (SPSS Inc., IL, USA). Data from experiments performed in triplicates are expressed as the mean ± SD. The Chi-square test was used for the comparison of patient characteristics. Student's t-test or Mann-Whitney U test was used for comparing means between two groups, while one-way ANOVA was used for more groups. The effect of HOXC10 expression on survival outcome was evaluated by the Kaplan-Meier method and subjected to a log-rank test. Association between clinicopathological factors, including HOXC10 expression, and survival outcomes of patients in clinical cohort 2 were estimated by univariate and multivariate Cox proportional hazards models. A p-value <0.05 was considered statistically significant.

Results

HOXC10 is upregulated in primary GC and related to poor survival outcomes. In our previous study, we showed that the expression of HOXC10 was markedly altered in GC tissues using cDNA microarray [16]. Here, we first examined the expression of HOXC10 in GC and matched adjacent non-tumor tissues (clinical cohort 1, n=70). The results showed a significant increase in the expression of HOXC10

mRNA in primary GC tissues (average fold change 22.88, p<0.01) (Figure 1A). In addition, HOXC10 protein expression was consistently upregulated in the representative GC tissues (n=8) (Figure 1B).

To explore whether the expression of HOXC10 is related to GC progression, tissue immunohistochemistry microarray analysis was performed in clinical cohort 2 (n=195, including 150 GC and adjacent non-tumor tissue pairs and 45 individual GC tissues). The results confirmed the upregulation of HOXC10 in GC tissues (91.3%, 137/150, p<0.01) (Figures 1C, 1D). Kaplan-Meier survival analysis indicated that high expression of HOXC10 was related to the poor prognosis in GC patients (HR=2.223; 95% CI: 1.361–4.186) (Figure 1E). Univariate COX regression analysis identified that deeper infiltration, lymphatic and distant metastasis, late tumor stage, and high expression of HOXC10 were poor prognostic factors for GC patients (p<0.01) (Figure 1G, Supplementary Table S1). Multivariable analysis showed that HOXC10 expression was an independent predictor of survival (HR=1.863; 95% CI: 1.076–3.225) (Figure 1H, Supplementary Table S1).

In addition, bioinformatic analysis on the online GC database was performed to determine the clinical significance of HOXC10 in GC progression. We searched for differentially expressed HOX genes in The Cancer Genome Atlas (TCGA) database and observed that HOXC10 mRNA was the most obvious alteration, 122-fold higher in GC tissues than that in non-tumor tissues (n=33, p<0.01) (Supplementary Table S2). KM-plotter database of GC (http://www.kmplot.com) indicated that high HOXC10 expression was associated with poor survival outcome (n=876, HR=1.8; 95% CI: 1.5–2.16, Figure 1F). Taken together, the expression of HOXC10 was upregulated in GC tissues and related to poor patient prognosis.

HOXC10 promotes GC growth *in vitro* and *in vivo*. We next investigated the functional role of HOXC10 on cell proliferation in a panel of GC cell lines (Figure 2A, Supplementary Figure S1). Both, the cell growth curve and colony formation assays showed that stable overexpression of HOXC10 significantly promoted cell proliferation (MKN28 and AGS) (Figures 2B, 2C). Consistently, forced expression of HOXC10 resulted in a higher proportion of cells with potent DNA replication abilities as indicated by EdU cell proliferation assays (Figure 2D). In contrast, knocking down HOXC10 suppressed cell proliferation in both BGC823 and SGC7901 cell lines (Figures 2B, 2C). In addition, we performed Transwell assays in GC cells with altered HOXC10 expression. Results showed that the overexpression of HOXC10 (AGS and MKN28) enhanced, whereas the knockdown of HOXC10 (BGC823 and SGC7901) suppressed cell migration (Figures 2E, 2F). Similar effects were also observed in Transwell cell invasion assays. The invasion ability of GC cells was enhanced with HOXC10 overexpression (AGS) and diminished with HOXC10 knockdown (BGC823 and SGC7901) (Supplementary Figure S2).

The effects of HOXC10 on GC growth were further evaluated *in vivo*. MKN28 cells overexpressing HOXC10 or SGC7901 cells with HOXC10 knocked down were subcutaneously injected into nude mice. Ectopic expression of HOXC10 accelerated GC tumor growth. Conversely, the knockdown of HOXC10 suppressed tumor formation (Figure 3E). Immunohistochemical analysis showed more Ki-67-positive stained cells in the HOXC10 overexpression group, whereas fewer stained cells in the HOXC10 knockdown group (Figure 3F).

HOXC10 regulates the G1/S cell cycle transition. To elucidate the mechanism underlying the effect of HOXC10 on cell proliferation, the cell cycle assays were performed using flow cytometry. The results illustrated that overexpression of HOXC10 significantly promoted the G1/S cell cycle transition (Figure 3A), whereas knocking down HOXC10 induced cell cycle arrest at the G1 phase (Figure 3B). To reduce the impact of cell cycle asynchrony on cell cycle distribution, the synchronization drug nocodazole was then used to block the GC cells at the G2/M phase. The results indicated that there were significantly more GC cells at the G1 phase when HOXC10 was knocked down at baseline. With the release of the G2/M blocker, the differences in the G1 phase between the HOXC10-depleted and control shRNA groups gradually narrowed. The results confirmed that knocking down HOXC10 induced GC cell cycle arrest at the G1 phase (Figure 3C).

Key G1/S cell cycle regulators, including CDK2 and p21, were evaluated in HOXC10-depleted cells. As expected, knocking down HOXC10 resulted in the upregulation of p21, as well as reduced CDK2 expression. In addition, the expression of c-Myc, a key factor in the G1/S cell cycle transition pathway [22], also decreased in HOXC10-knockdown cells (Figure 3D). Collectively, these results showed that HOXC10 promoted GC cell proliferation by accelerating the G1/S cell cycle transition.

HOXC10 represses the transcriptional activity of p21. To identify potential downstream genes of HOXC10, a genome-wide analysis of BGC823 cells transfected with siRNA targeting HOXC10 was conducted. The results showed that numerous genes were differentially regulated by knocking down HOXC10 (Table 1). We confirmed the differential expression of nine selected genes, including p21, by qPCR analysis in HOXC10-depleted cells (Figure 4A). Results showed that the knocking down of HOXC10 promoted the expression of p21. As expected, the p21 protein was inversely regulated by HOXC10 in GC cell lines (Figure 4B). Immunohistochemical staining showed that the HOXC10-overexpressing nude mice exhibited reduced p21 expression (Figure 4C). Furthermore, TCGA database (n=439) shows a negative correlation between HOXC10 and p21 in GC tissues (Pearson Correlation = –0.231, p<0.01) (Figure 4D).

We hypothesized that HOXC10 could transcriptionally repress the expression of p21. We searched the JASPAR (http://jaspar.genereg.net/) database and found several

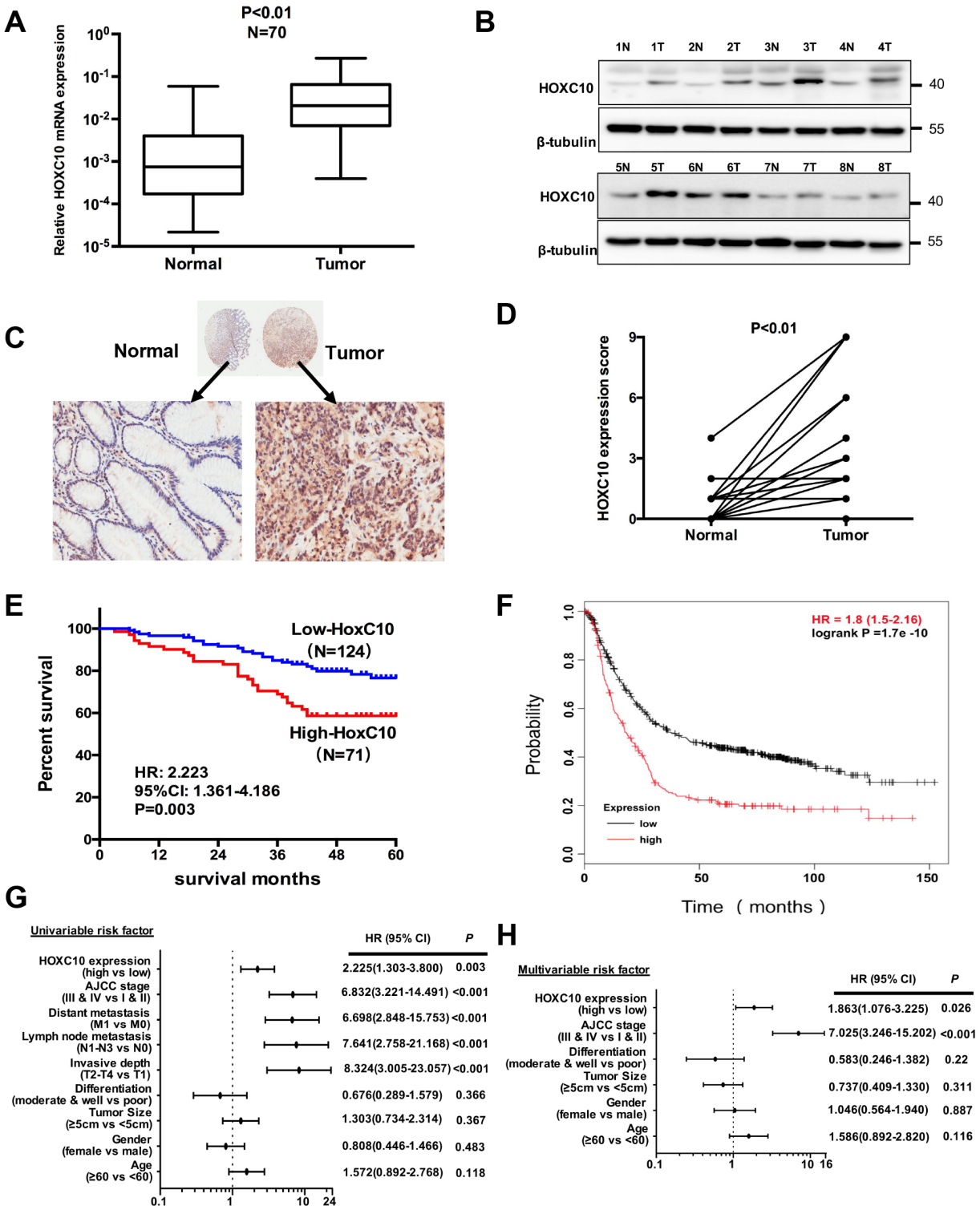

Figure 1. The expression of HOXC10 is upregulated in human gastric cancer (GC) and is related to poor survival. A) HOXC10 mRNA expression was measured in GC and matched non-tumor tissues in clinical cohort 1 (n=70, p<0.01). B) Representative results of the expression of HOXC10 protein in GC and non-tumor tissues (n=8). C) Representative diagram of HOXC10 immunohistochemical expression in human GC tissues microarray in clinical cohort 2. D) The quantification of HOXC10 expression in tissue microarray was implemented by immunohistochemistry score (n=150, p<0.01). E) Kaplan-Meier curves for disease-specific survival of GC patients classified by HOXC10 expression (n=195, HR=2.223; 95% CI: 1.361–4.186). F) Kaplan-Meier curves for relapse-free survival of GC patients classified by HOXC10 expression from KM-plotter database (n=876). G) Univariate analysis was performed in cohort 2. H) Multivariate analysis was performed in cohort 2. The bars correspond to 95% confidence intervals.

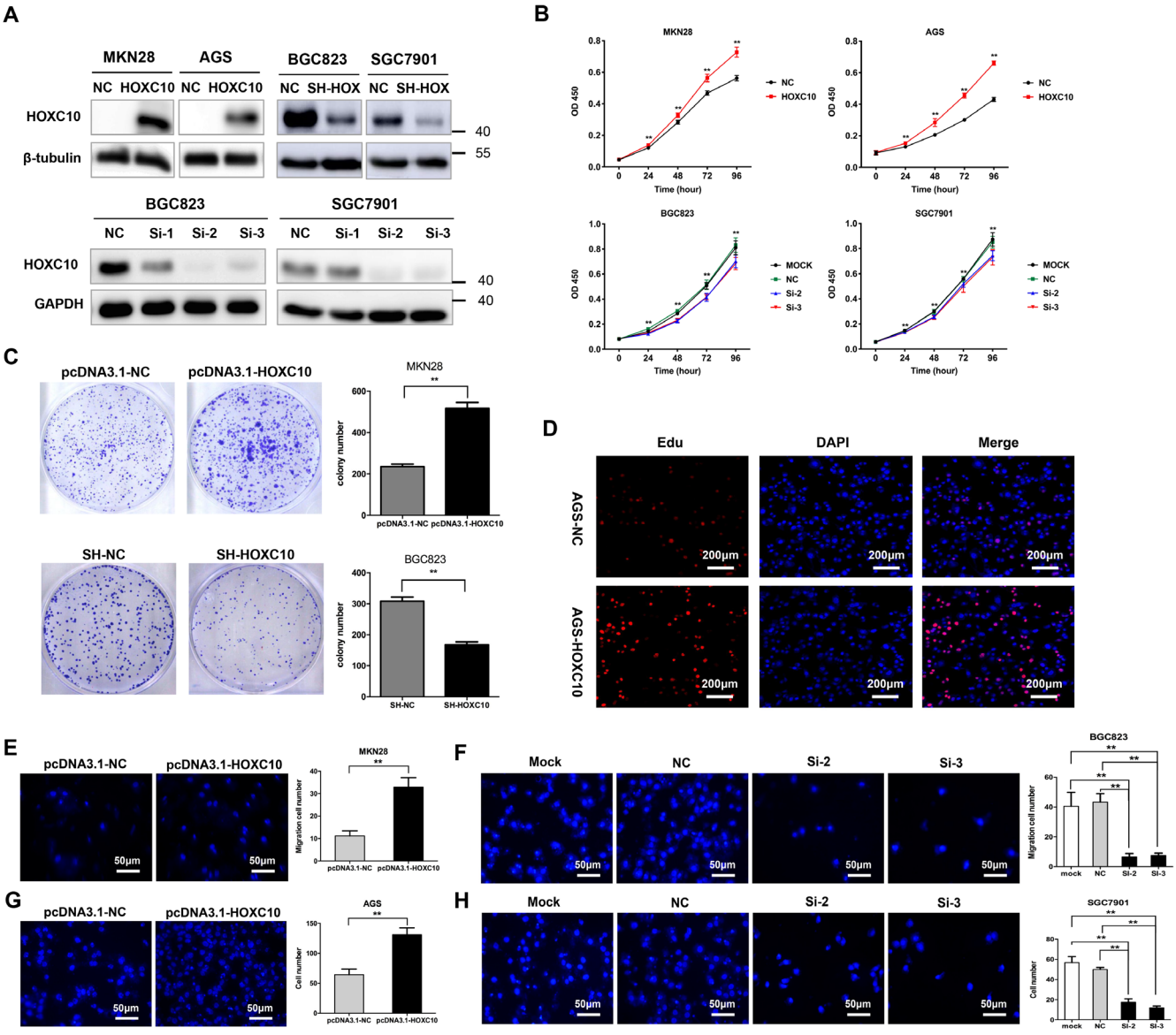

Figure 2. The effect of HOXC10 on gastric cancer cell proliferation and migration. A) The expression level of HOXC10 in GC cells transfected with pcDNA3.1-HOXC10 or HOXC10 siRNA/shRNA was confirmed by western blotting. Cell growth curve (B) and colony formation assays (C) indicated that the overexpression of HOXC10 induced a significant increase in MKN28 and AGS cell proliferation, whereas depletion of HOXC10 suppressed BGC823 and SGC7901 cell proliferation. D) AGS cells overexpressing HOXC10 showed a higher proportion of proliferative cells by EdU cell proliferation assays. Overexpression of HOXC10 enhanced MKN28 (E) and AGS (G) cell migration, whereas silencing of HOXC10 inhibited BGC823 (F) and SGC7901 (H) cell migration. *p<0.05, **p<0.01

potential HOXC10 binding sites in the promoter of p21 (the 2.5kb upstream sequence of p21) (Figure 4E). The region –2.5 kb to +180 bp of the p21 promoter, which includes HOXC10 binding sites, was cloned into a pGL3-basic vector. The dual-luciferase reporter assays showed that the overexpression of HOXC10 inhibited the transcriptional activity of p21(Figure 4F), whereas the knocking down of HOXC10 enhanced its activity (Figure 4H). We then investigated whether HOXC10 was physically bound to the p21 promoter. Further investigation using a ChIP assay with primers specific to the promoter regions of p21 indicated that HOXC10 could directly bind to the p21 promoter (Figure 4G). Collectively, our results illustrated that by binding to the promoter region of p21 the increased expression of HOXC10 in GC cells could inhibit the expression of p21 at the transcriptional level, and promote the expression of some critical regulators of G1/S cell cycle transition, such as CKD2 and c-Myc, resulting in the enhanced ability of GC cell proliferation (Figure 4I).

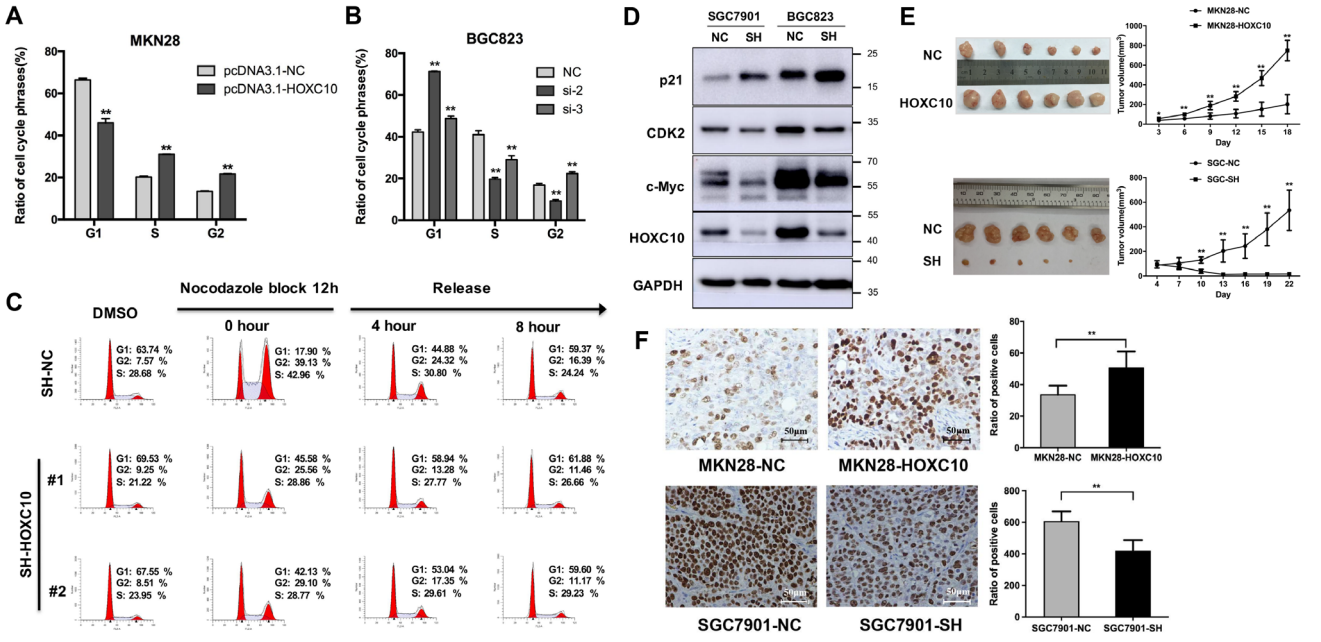

Figure 3. HOXC10 regulates the G1/S cell cycle transition and tumor growth *in vivo*. A) Flow cytometry showed that the overexpression of HOXC10 promoted the G1/S cell cycle transition. B) Silencing of HOXC10 induced cell cycle arrest at the G1 phase. C) Cell cycle distribution of BGC823 cells transfected with shRNA targeted HOXC10 or negative control shRNA was determined by flow cytometry. Cells were unsynchronized (DMSO treatment), synchronized using a G2/M blocker (nocodazole treatment), and then harvested at the indicated times after a release from the nocodazole block. D) Alterations in the expression of p21, CDK2, and c-Myc in HOXC10-silenced cells compared to control cells by western blotting. E) Tumors from nude mice. After implantation of HOXC10-overexpressing MKN28 cells or HOXC10-silencing SGC7901 cells and negative control cells, tumor volume was assessed every three days (data shown as mean ± SD). F) Immunohistochemical analysis of tumors from nude mice using the Ki-67 antibody and calculation of the number of Ki-67-positive cells. *p<0.05, **p<0.01

Table 1. Representative genes in HOXC10-depleted gastric cancer cells in comparison with negative control by cDNA microarray.

Gene Symbol	Gene description	Fold change	Regulation	Gene Function
ELF5	ETS-related transcription factor Elf-5 isoform 1	27.78	up	I, M, P[a]
SEMA6B	Semaphorin-6B precursor	8.39	up	Ad, I, M
UPK1A	Uroplakin 1A	6.24	up	CC, I, M, P
PRDM2	PR domain zinc finger protein 2 isoform d	3.32	up	Ap, CC, M, P
BAX	BCL2 associated X	3.07	up	Ap, P
FHL1	Four and a half LIM domains protein 1 isoform 5	2.80	up	Ad, CC, I, M, P
FOXO4	Forkhead box protein O4 isoform 1	2.45	up	I, M, Me, P
AKT3	RAC-gamma serine/threonine-protein kinase isoform 2	2.29	up	An, Ap, P
RASSF4	Ras association domain-containing protein 4	2.07	up	P
CDKN1A	Cyclin-dependent kinase inhibitor 1	1.33	up	Ap, CC, P
SLC39A10	Solute carrier family 39 member 10	27.51	down	I
RHOJ	Rho-related GTP-binding protein RhoJ precursor	11.01	down	An, Me, P
ZEB1	Zinc finger E-box-binding homeobox 1 isoform b	8.13	down	CC, I, M, Me, P
CCL25	C-C motif chemokine 25 isoform 1 precursor	5.16	down	I, M, P
NRP2	Neuropilin-2 isoform 6 precursor	4.83	down	An, Ap, Me
CXCL9	C-X-C motif chemokine 9 precursor	2.32	down	Ap, I, M, Me, P

Abbreviations: Ad-adhesion; An-angiogenesis; Ap-apoptosis; CC-cell cycle; I-invasion; M-migration; Me-metastasis; P-proliferation

Discussion

The present study revealed that the expression of HOXC10 was upregulated in GC tissues from two clinical cohorts and TCGA database, and served as an independent prognostic factor of patients. The aberrant expression of HOXC10 has been reported in different human cancers and correlated with poor prognosis. Kim et al. [15] have revealed that HOXC10 is overexpressed in GC tissues which is based solely on database analysis. Our previous study has demonstrated that high expression of HOXC10 in GC is associated with poor

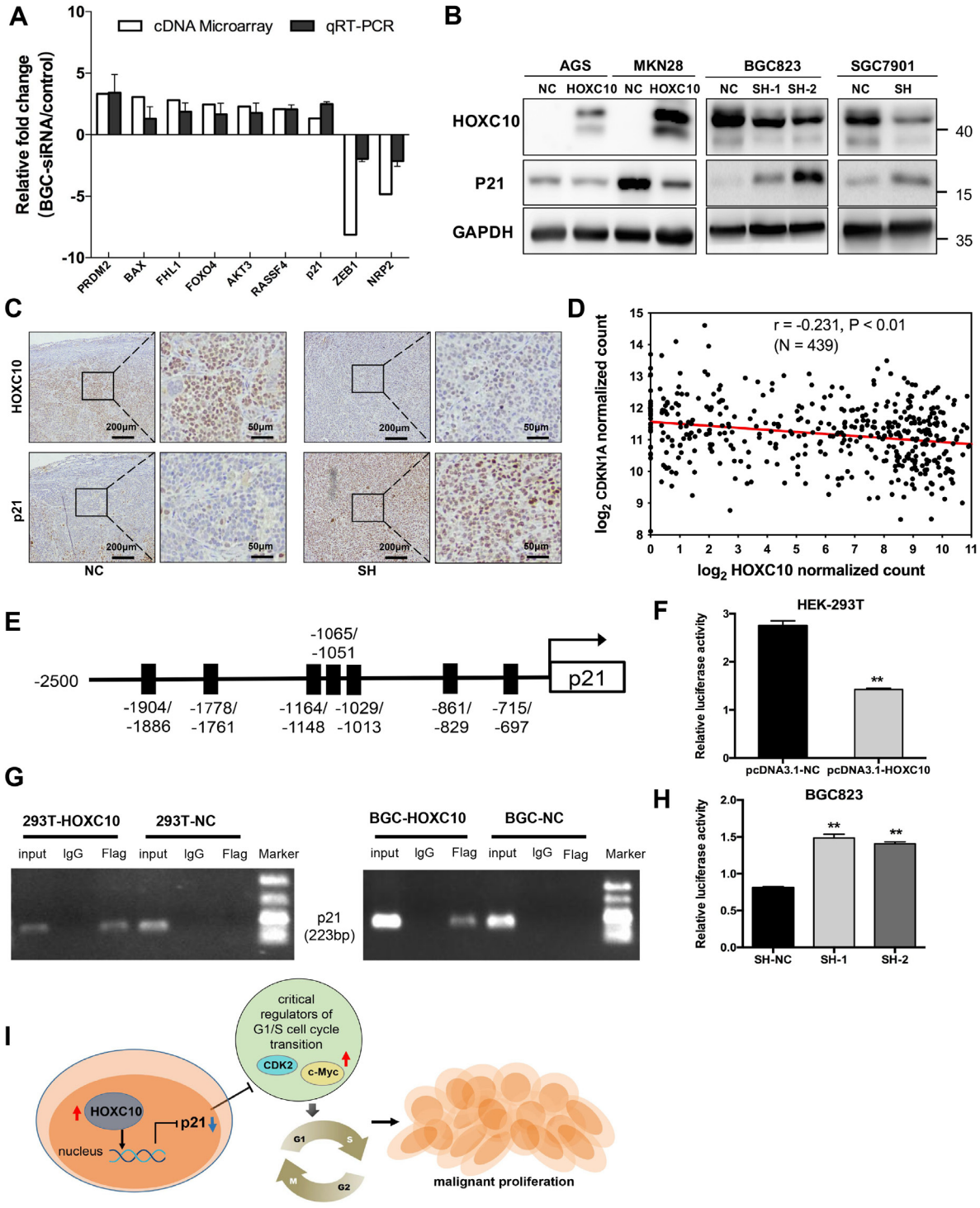

Figure 4. HOXC10 inhibits p21 transcription and binds to the p21 promoter. The expression levels of nine selected genes in HOXC10-depleted BGC823 cells were detected by qPCR (data shown as mean ± SD). B) The protein levels of HOXC10 and p21 in gastric cancer cells after overexpression or silenced expression of HOXC10. C) Representative immunohistochemistry of HOXC10 (upper) and p21 (lower) proteins in subcutaneous xenografts from nude mice with or without HOXC10 depletion. D) Negative correlation between HOXC10 and p21 was found in GC tissues from TCGA database by Pearson Correlation analysis (r=–0.231, n=439, p<0.01). E) Schematic diagram of the potential HOXC10-binding sites in the p21 promoter. F) Overexpression of HOXC10 repressed the transcriptional activity of p21. G) Direct binding of HOXC10 protein to the p21 promoter was validated by ChIP assay. Protein-DNA complexes were immunoprecipitated using Flag-specific antibody in HEK-293T and BGC823 cells overexpressing Flag-tagged HOXC10. H) Knocking down of HOXC10 enhanced the transcriptional activity of p21. I) Proposed mechanism in which HOXC10 promotes G1/S cell cycle transition and proliferation in gastric cancer. **p<0.01

prognosis, but the sample size is small and needs to be further confirmed by expanding the specimen [23]. The upregulation of HOXC10 has been associated with poor survival in patients with estrogen receptor-negative breast cancer. A more significant upregulation has also been reported in distant metastasis arising after failed chemotherapy [18].

To clarify the clinical value of HOXC10 in GC, we also investigated the correlation of HOXC10 expression in GC tissues with clinicopathological features. In clinical cohort 1, the mRNA level of HOXC10 in GC tissues was correlated with tumor size, depth of invasion, lymph node metastasis, and tumor staging ($p<0.01$, Supplementary Table S3). In clinical cohort 2, the protein expression of HOXC10 was significantly correlated with the gender, depth of tumor invasion, and tumor staging ($p<0.05$, Supplementary Table S4). The statistical differences in the correlation between gender, tumor size, lymph node metastasis, and HOXC10 expression may be caused by different sample sizes and detection levels. However, these results strongly suggest that HOXC10 expression is related to specific clinicopathological features of GC, such as depth of tumor invasion and tumor staging. Using clinical and online GC databases, the correlation between high HOXC10 expression and poor prognosis was also confirmed. These results suggest that HOXC10 is expected to be a candidate biomarker for GC progression and a target for individualized therapy.

HOXC10 is mainly involved in human embryonic development. However, the functional role of HOXC10 in cancers remains controversial. Yali et al. [24] identified HOXC10 as an important mediator of invasion through gene expression profiling of tissue samples, including normal, high-grade squamous intraepithelial lesions, and cervical squamous cell carcinomas. Overexpression of HOXC10 promotes cervical cancer cell colony formation and cell proliferation [25]. A previous study demonstrated that overexpressed HOXC10 induced by IL-1β promotes hepatocellular carcinoma metastasis by transactivating PDPK1 and VASP expression [26]. Intriguingly, a study revealed that reduced HOXC10 in breast cancer cells increased cell growth, decreased apoptosis, enhanced cell migration, and contributed to antiestrogen resistance *in vitro* and *in vivo*, suggesting HOXC10 is a growth-inhibiting gene [27]. This discrepancy might be due to the differences in cell type and tumor microenvironment.

Our study demonstrated that HOXC10 plays an 'oncogenic' role in GC. Enforced expression of HOXC10 could promote cell proliferation, invasion, and tumorigenesis. This is consistent with a recent study that has shown that HOXC10 enhances GC cell viability and invasion [13, 15]. Nevertheless, previous studies failed to elucidate the specific molecular mechanisms by which HOXC10 accelerates GC cell proliferation. Malignant cells release mitogenic signals that regulate the properties of the cell cycle and cell survival, by which they acquire the capability to activate proliferation. Davide et al. [28] revealed that HOXC10 dynamically altered mitosis and influenced cell cycle progression in Hela cells. We found that the overexpression of HOXC10 promoted the GC cell G1/S phase transition. Consistently, a study showed that the overexpression of HOXC10 promoted cell proliferation and G1/S cell cycle transition in breast cancer cells [18]. Those findings suggest that HOXC10 might be involved in the development of various cancers by controlling the cell cycle.

HOX proteins act as transcriptional factors and contain a common DNA-binding domain called the homeodomain [29, 30]. Haiyan et al. [31] identified five target genes of HOXC8 in mouse embryo fibroblast cells containing HOX consensus DNA-binding sequences. In breast cancer cells, HOXC10 could bind to and activate CDK7, thus facilitating DNA damage repair [18]. We found that the depletion of HOXC10 reduced the expression of several key regulators in the G1/S cell cycle transition, including p21, CDK2, and c-Myc. Importantly, HOXC10 repressed the activity of p21 transcription by binding to its promoter. A previous study showed that knocking down HOXA10 in oral cancer cells was accompanied by a reduction in cell proliferation and an increase in p21 expression [32]. By potently inhibiting CDKs, p21 exerts critical functions in cell cycle control and constitutes a G1 cell cycle checkpoint [20]. Overexpression of p21 in malignant cells inhibits tumorigenesis via cell cycle arrest and apoptosis induction [33–35]. Mutations in the coding region of the p21 gene were rarely found in cancer cells, whereas epigenetic regulation, such as DNA methylation and histone acetylation, may represent an alternative mechanism by which the transcription of p21 is inhibited [36]. It has been reported that HOX proteins can recruit histone deacetylases as transcriptional corepressors that mediate the transcriptional repression activity [37, 38]. HOXC10 may thus repress the transcription of p21 by interacting with co-factors, such as histone deacetylases, thereby warranting further investigations.

In conclusion, we demonstrated the upregulation of HOXC10 in GC tissues and defined HOXC10 as an independent predictor of survival for GC patients. We also highlighted the functional importance of HOXC10 in the GC cell cycle control and growth induction through transcriptional repression of p21. Therefore, the present study suggests that HOXC10 acts as a prognostic biomarker and may be a potential therapeutic target in GC.

Supplementary information is available in the online version of the paper.

Acknowledgments: This work was supported by grants from the National Natural Science Foundation of China (81802348 and 81972671).

References

[1] SUNG H, FERLAY J, SIEGEL RL, LAVERSANNE M, SOERJOMATARAM I et al. Global Cancer Statistics 2020: GLOBOCAN Estimates of Incidence and Mortality Worldwide for 36 Cancers in 185 Countries. CA Cancer J Clin 2021; 71: 209–249. https://doi.org/10.3322/caac.21660

[2] KAMANGAR F, DORES GM, ANDERSON WF. Patterns of cancer incidence, mortality, and prevalence across five continents: defining priorities to reduce cancer disparities in different geographic regions of the world. J Clin Oncol 2006; 24: 2137–2150. https://doi.org/10.1200/JCO.2005.05.2308

[3] WONG SS, KIM KM, TING JC, YU K, FU J et al. Genomic landscape and genetic heterogeneity in gastric adenocarcinoma revealed by whole-genome sequencing. Nat Commun 2014; 5: 5477. https://doi.org/10.1038/ncomms6477

[4] MCGINNIS W, LEVINE MS, HAFEN E, KUROIWA A, GEHRING WJ. A conserved DNA sequence in homoeotic genes of the Drosophila Antennapedia and bithorax complexes. Nature 1984; 308: 428–433. https://doi.org/10.1038/308428a0

[5] ABATE-SHEN C. Deregulated homeobox gene expression in cancer: cause or consequence? Nat Rev Cancer 2002; 2: 777–785. https://doi.org/10.1038/nrc907

[6] DE BESSA GARCIA SA, ARAUJO M, PEREIRA T, MOUTA J, FREITAS R. HOX genes function in Breast Cancer development. Biochim Biophys Acta Rev Cancer 2020; 1873: 188358. https://doi.org/10.1016/j.bbcan.2020.188358

[7] FENG W, HUANG W, CHEN J, QIAO C, LIU D et al. CXCL12-mediated HOXB5 overexpression facilitates Colorectal Cancer metastasis through transactivating CXCR4 and ITGB3. Theranostics 2021; 11: 2612–2633. https://doi.org/10.7150/thno.52199

[8] HE Q, HUANG W, LIU D, ZHANG T, WANG Y et al. Homeobox B5 promotes metastasis and poor prognosis in Hepatocellular Carcinoma, via FGFR4 and CXCL1 upregulation. Theranostics 2021; 11: 5759–5777. https://doi.org/10.7150/thno.57659

[9] XU F, SHANGGUAN X, PAN J, YUE Z, SHEN K et al. HOXD13 suppresses prostate cancer metastasis and BMP4-induced epithelial-mesenchymal transition by inhibiting SMAD1. International journal of cancer. Int J Cancer 2021; 148: 3060–3070. https://doi.org/10.1002/ijc.33494

[10] LI L, ZHANG X, LIU Q, YIN H, DIAO Y et al. Emerging role of HOX genes and their related long noncoding RNAs in lung cancer. Crit Rev Oncol Hematol 2019; 139: 1–6. https://doi.org/10.1016/j.critrevonc.2019.04.019

[11] ZHANG Q, JIN XS, YANG ZY, WEI M, LIU BY et al. Upregulated Hoxc6 expression is associated with poor survival in gastric cancer patients. Neoplasma 2013; 60: 439–445. https://doi.org/10.4149/neo_2013_057

[12] WANG L, CHEN S, XUE M, ZHONG J, WANG X et al. Homeobox D10 gene, a candidate tumor suppressor, is downregulated through promoter hypermethylation and associated with gastric carcinogenesis. Mol Med 2012; 18: 389–400. https://doi.org/10.2119/molmed.2011.00172

[13] GUO C, HOU J, AO S, DENG X, LYU G. HOXC10 upregulation promotes gastric cancer cell proliferation and metastasis through MAPK pathway. Chin J Cancer Res 2017; 29: 572–580. https://doi.org/10.21147/j.issn.1000-9604.2017.06.12

[14] YAO S, HE L, ZHANG Y, YE L, LAI Y et al. HOXC10 promotes gastric cancer cell invasion and migration via regulation of the NF-kappaB pathway. Biochem Biophys Res Commun 2018; 501: 628–635. https://doi.org/10.1016/j.bbrc.2018.05.019

[15] KIM J, BAE DH, KIM JH, SONG KS, KIM YS et al. HOXC10 overexpression promotes cell proliferation and migration in gastric cancer. Oncol Rep 2019; 42: 202–212. https://doi.org/10.3892/or.2019.7164

[16] ZHAO Y, ZHOU T, LI A, YAO H, HE F et al. A Potential Role of Collagens Expression in Distinguishing Between Premalignant and Malignant Lesions in Stomach. Anat Rec (Hoboken) 2009; 292: 692–700. https://doi.org/10.1002/ar.20874

[17] SHAH N, SUKUMAR S. The Hox genes and their roles in oncogenesis. Nat Rev Cancer 2010; 10: 361–371. https://doi.org/10.1038/nrc2826

[18] SADIK H, KORANGATH P, NGUYEN NK, GYORFFY B, KUMAR R et al. HOXC10 Expression Supports the Development of Chemotherapy Resistance by Fine Tuning DNA Repair in Breast Cancer Cells. Cancer Res 2016; 76: 4443–4456. https://doi.org/10.1158/0008-5472.CAN-16-0774

[19] GEORGAKILAS AG, MARTIN OA, BONNER WM. p21: A Two-Faced Genome Guardian. Trends Mol Med 2017; 23: 310–319. https://doi.org/10.1016/j.molmed.2017.02.001

[20] HARPER JW, ADAMI GR, WEI N, KEYOMARSI K, ELLEDGE SJ. The p21 Cdk-interacting protein Cip1 is a potent inhibitor of G1 cyclin-dependent kinases. Cell 1993; 75: 805–816. https://doi.org/10.1016/0092-8674(93)90499-g

[21] KREIS NN, LOUWEN F, YUAN J. The Multifaceted p21 (Cip1/Waf1/CDKN1A) in Cell Differentiation, Migration and Cancer Therapy. Cancers (Basel) 2019; 11: 1220. https://doi.org/10.3390/cancers11091220

[22] LIM S, KALDIS P. Cdks, cyclins and CKIs: roles beyond cell cycle regulation. Development 2013; 140: 3079–3093. https://doi.org/10.1242/dev.091744

[23] HE J, GE Q, LIN Z, SHEN W, LIN R et al. MiR-129-5p induces cell cycle arrest through modulating HOXC10/Cyclin D1 to inhibit gastric cancer progression. FASEB J 2020; 34: 8544–8557. https://doi.org/10.1096/fj.201903217R

[24] ZHAI Y, KUICK R, NAN B, OTA I, WEISS SJ et al. Gene expression analysis of preinvasive and invasive cervical squamous cell carcinomas identifies HOXC10 as a key mediator of invasion. Cancer Res 2007; 67: 10163–10172. https://doi.org/10.1158/0008-5472.CAN-07-2056

[25] ZHAI Y, KUICK R, NAN B, OTA I, WEISS SJ et al. Gene Expression Analysis of Preinvasive and Invasive Cervical Squamous Cell Carcinomas Identifies HOXC10 as a Key Mediator of Invasion. Cancer Res 2007; 67: 10163–10172. https://doi.org/10.1158/0008-5472.can-07-2056

[26] DANG Y, CHEN J, FENG W, QIAO C, HAN W et al. Interleukin 1beta-mediated HOXC10 Overexpression Promotes Hepatocellular Carcinoma Metastasis by Upregulating PDPK1 and VASP. Theranostics 2020; 10: 3833–3848. https://doi.org/10.7150/thno.41712

[27] PATHIRAJA TN, NAYAK SR, XI Y, JIANG S, GAREE JP et al. Epigenetic reprogramming of HOXC10 in endocrine-resistant breast cancer. Sci Transl Med 2014; 6: 229ra241. https://doi.org/10.1126/scitranslmed.3008326

[28] GABELLINI D, COLALUCA IN, VODERMAIER HC, BIAMONTI G, GIACCA M et al. Early mitotic degradation of the homeoprotein HOXC10 is potentially linked to cell cycle progression. Embo J 2003; 22: 3715–3724. https://doi.org/10.1093/Emboj/Cdg340

[29] MCGINNIS W, KRUMLAUF R. Homeobox genes and axial patterning. Cell 1992; 68: 283–302. https://doi.org/10.1016/0092-8674(92)90471-n

[30] RUDDLE FH, BARTELS JL, BENTLEY KL, KAPPEN C, MURTHA MT et al. Evolution of Hox genes. Annu Rev Genet 1994; 28: 423–442. https://doi.org/10.1146/annurev.ge.28.120194.002231

[31] LEI H, JUAN AH, KIM MS, RUDDLE FH. Identification of a Hoxc8-regulated transcriptional network in mouse embryo fibroblast cells. Proc Natl Acad Sci U S A 2006; 103: 10305–10309. https://doi.org/10.1073/pnas.0603552103

[32] CARRERA M, BITU CC, DE OLIVEIRA CE, CERVIGNE NK, GRANER E et al. HOXA10 controls proliferation, migration and invasion in oral squamous cell carcinoma. Int J Clin Exp Pathol 2015; 8: 3613–3623.

[33] HRGOVIC I, DOLL M, KLEEMANN J, WANG XF, ZOELLER N et al. The histone deacetylase inhibitor trichostatin a decreases lymphangiogenesis by inducing apoptosis and cell cycle arrest via p21-dependent pathways. Bmc Cancer 2016; 16: 763. https://doi.org/10.1186/s12885-016-2807-y

[34] VALESKY EM, HRGOVIC I, DOLL M, WANG XF, PINTER A et al. Dimethylfumarate effectively inhibits lymphangiogenesis via p21 induction and G1 cell cycle arrest. Exp Dermatol 2016; 25: 200–205. https://doi.org/10.1111/exd.12907

[35] LIU YW, XIA R, LU K, XIE M, YANG F et al. LincRNAFEZF1-AS1 represses p21 expression to promote gastric cancer proliferation through LSD1-Mediated H3K-4me2 demethylation. Mol Cancer 2017; 16: 39. https://doi.org/10.1186/s12943-017-0588-9

[36] FANG JY, LU YY. Effects of histone acetylation and DNA methylation on p21(WAF1) regulation. World J Gastroenterol 2002; 8: 400–405. https://doi.org/10.3748/wjg.v8.i3.400

[37] LU Y, GOLDENBERG I, BEI L, ANDREJIC J, EKLUND EA. HoxA10 represses gene transcription in undifferentiated myeloid cells by interaction with histone deacetylase 2. J Biol Chem 2003; 278: 47792–47802. https://doi.org/10.1074/jbc.M305885200

[38] SALEH M, RAMBALDI I, YANG XJ, FEATHERSTONE MS. Cell signaling switches HOX-PBX complexes from repressors to activators of transcription mediated by histone deacetylases and histone acetyltransferases. Mol Cell Biol 2000; 20: 8623–8633. https://doi.org/10.1128/Mcb.20.22.8623-8633.2000

[39] XUE M, FANG Y, SUN G, ZHUO W, ZHONG J et al. IGFBP3, a transcriptional target of homeobox D10, is correlated with the prognosis of gastric cancer. PLoS One 2013; 8: e81423. https://doi.org/10.1371/journal.pone.0081423

https://doi.org/10.4149/neo_2022_220609N615

HOXC10 indicates poor survival outcome in gastric cancer and promotes G1/S cell cycle transition through transcriptional repression of p21

Zheng-Hua LIN[1,2,3], Jia-Min HE[2,4], San-Chuan LAI[1,2,3], Ning DING[1,2,3], Ying JIANG[1], Xing-Kang HE[2,4], Xiao-Sun LIU[5], Zhi-Hui HUANG[4,*]

Supplementary Information

Supplementary Table S1. Association between clinicopathological factors and survival outcomes of patients in clinical cohort 2*: univariate and multivariate Cox proportional hazards models.

Variable	Univariate Cox regression			Multivariate Cox regression		
	HR	95% CI	p-value	HR	95% CI	p-value
Age						
<60	1			1		
≥60	1.572	0.892–2.768	0.118	1.586	0.892–2.820	0.116
Gender						
Male	1			1		
Female	0.808	0.446–1.466	0.483	1.046	0.564–1.940	0.887
Tumor Size						
<5 cm*5 cm	1			1		
≥5 cm*5 cm	1.303	0.734–2.314	0.367	0.737	0.409–1.330	0.311
Differentiation						
Poor	1			1		
Moderate/High	0.676	0.289–1.579	0.366	0.583	0.246–1.382	0.22
Invasive depth						
T1	1					
T2–T4	8.324	3.005–23.057	< 0.001			
Lymph node metastasis						
N0	1					
N1–N3	7.641	2.758–21.168	< 0.001			
Distant metastasis						
M0	1					
M1	6.698	2.848–15.753	< 0.001			
Stage (TNM)						
I–II	1			1		
III–IV	6.832	3.221–14.491	< 0.001	7.025	3.246–15.202	< 0.001
HoxC10 expression						
Low[a]	1			1		
High[b]	2.225	1.303–3.800	0.003	1.863	1.076–3.225	0.026

Notes: *clinical cohort 2: clinical cohort from the First Affiliated Hospital of Zhejiang University; [a]0 < IHC score ≤ 2; [b]2 < IHC score ≤ 9

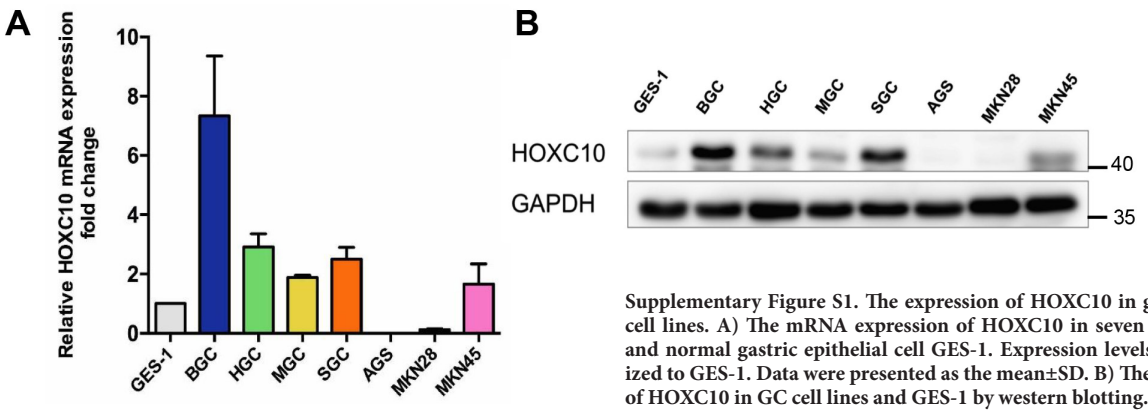

Supplementary Figure S1. The expression of HOXC10 in gastric cancer cell lines. A) The mRNA expression of HOXC10 in seven GC cell lines and normal gastric epithelial cell GES-1. Expression levels are normalized to GES-1. Data were presented as the mean±SD. B) The protein level of HOXC10 in GC cell lines and GES-1 by western blotting.

Supplementary Table S2. The differential expressed HOX genes in the Cancer Genome Atlas (TCGA) database.

Gene	Fold Change	Log2 Fold Change	Adjusted p-value
HOXC10	122.2189598	6.933324298	2.4413E-25
HOXA11	41.07898788	5.360328731	7.98901E-11
HOXC13	37.54748328	5.230644305	0.000189743
HOXC11	36.89485295	5.205347661	1.49748E-22
HOXC9	19.20318991	4.263274077	3.2387E-11
HOXA10	14.87340081	3.894662653	4.01616E-15
HOXC8	14.39354696	3.84735025	6.20946E-08
HOXA13	10.03742673	3.327317551	4.32547E-08
HOXA9	8.116636586	3.02088202	0.001351397
HOXB9	5.849739544	2.548372391	3.97657E-05
HOXC6	3.858573461	1.948067573	0.00026068
HOXB13	2.536115374	1.342620378	0.015197133
HOXB7	2.472743391	1.306112532	0.021266939
HOXA4	0.242617213	-2.043246185	1.29389E-05
HOXA2	0.330866644	-1.595678238	0.001161673
HOXA5	0.418968906	-1.255084918	0.011603545

Supplementary Table S3. Correlation between HOXC10 mRNA expression level and clinicopathological features in patients from clinical cohort 1*.

Clinicopathologic features	N=70	HoxC10 mRNA expression (T)	p-value
Age			0.603
<60	24	0.043526932	
≥60	46	0.044844822	
Gender			0.431
Male	49	0.039188458	
Female	21	0.056536846	
Tumor Size			0.007
<5 cm*5 cm	35	0.033176551	
≥5 cm*5 cm	35	0.055609398	
Differentiation			0.686
Poor	45	0.04712772	
Moderate/High	25	0.039470433	
Distant metastasis			0.272
M0	66	0.043843867	
M1	4	0.053453253	
Lymph node metastasis			0.002
N0	30	0.021164682	
N1-N3	40	0.061814194	
Invasive depth			<0.001
T0	18	0.010867083	
T1-T4	52	0.05599809	
Stage (TNM)			<0.001
I	21	0.013831959	
II	12	0.032293864	
III	33	0.067142354	
IV	4	0.053453253	

Notes: *clinical cohort 1: clinical cohort from the Sir Run Run Shaw Hospital of Zhejiang University

Supplementary Table S4. Correlation between HOXC10 expression and clinicopathological features in patients from clinical cohort 2*.

Clinicopathologic features	HoxC10 expression in nucleus		p-value
	Low (n=124)	High (n=71)	
Age			0.281
<60	57 (67.9)	27 (32.1)	
≥60	67 (60.4)	44 (39.6)	
Gender			0.003
Male	74 (56.5)	57 (43.5)	
Female	50 (78.1)	14 (21.9)	
Tumor Size			0.910
<5 cm*5 cm	90 (63.8)	51 (36.2)	
≥5 cm*5 cm	34 (63.0)	20 (37.0)	
Differentiation			0.854
Poor	106 (63.9)	60 (36.1)	
Moderate/High	18 (62.1)	11 (37.9)	
Invasive depth			0.005
T1	53 (76.8)	16 (23.2)	
T2–T4	71 (56.3)	55 (43.7)	
Lymph node metastasis			0.058
N0	48 (72.7)	18 (27.3)	
N1–N3	76 (58.9)	53 (41.1)	
Distant metastasis			0.259
M0	121 (64.4)	67 (35.6)	
M1	3 (42.9)	4 (57.1)	
Stage (TNM)			0.024
I	35 (81.4)	8 (18.6)	
II	32 (62.7)	19 (37.3)	
III	54 (58.1)	39 (41.9)	
IV	3 (37.5)	5 (62.5)	

Notes: *clinical cohort 2: clinical cohort from the First Affiliated Hospital of Zhejiang University

Supplementary Table S5. The sequences of the primers used in the study.

Gene	Primer	Sequence, 5'–3'
HOXC10	Forward	AGTGTGGCTGGTGTGTGTGT
	Reverse	AACGATTCTGCCTGTGCTCT
snRNA U6	Forward	CTCGCTTCGGCAGCACA
	Reverse	AACGCTTCACGAATTTGCGT
GAPDH	Forward	GAAGGTGAAGGTCGGAGT
	Reverse	GAAGATGGTGATGGGATTTC
P21(CDKN1A)	Forward	GGAAGGGACACACAAGAAGAAG
	Reverse	AGCCTCTACTGCCACCATCTTA
AKT3	Forward	GGATGCCTCTACAACCCATC
	Reverse	CCACTTGCCTTCTCTCGAAC
BAX	Forward	TCTGACGGCAACTTCAACTG
	Reverse	GGTGAGGAGGCTTGAGGAGT
FHL1	Forward	ATGGCGGAGAAGTTTGACTG
	Reverse	CACAGGTGTTGGCACAGAAC
FOXO4	Forward	TGGTTCCCACCCTTTCTATG
	Reverse	CATTCTGTCTTGGCTTGCAG
RASSF4	Forward	CCGTGTTTACTCCAGCCTATG
	Reverse	GGCCATCTTCCACCCTAAAT
PROM2	Forward	GGGCCATTTGTTGGTGATAA
	Reverse	TCCCTTCTCTGGATCAGTGG
NRP2	Forward	ACCTGGAGCATGACCCTTTG
	Reverse	GAGGATCCCCGTCGATGAAC
ZEB1	Forward	GTGTAAGCGCAGAAAGCAGG
	Reverse	TGGTCTGTTGGCAGGTCATC

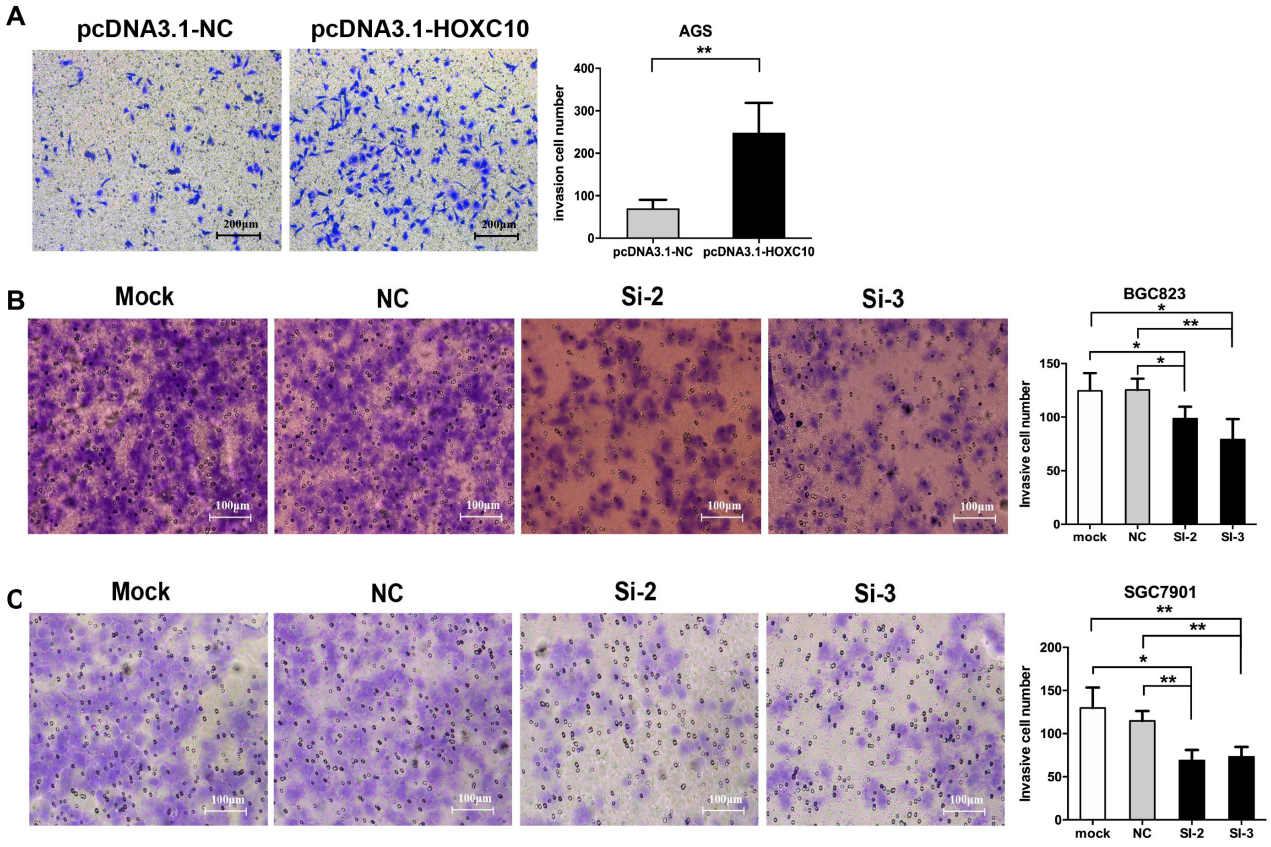

Supplementary Figure S2. The expression of HOXC10 in gastric cancer cell lines. A) Overexpression of HOXC10 enhanced AGS cell invasion, whereas silencing of HOXC10 suppressed cell invasive ability in BGC823 (B) and SGC7901 (C) cells. *p<0.05, **p<0.01